Solar Energy Vol. 38, No. 6, pp. 437–446, 1987
Printed in the U.S.A.

0038–092X/87 $3.00 + .00
Pergamon Journals Ltd.

MEASUREMENT OF INTERZONAL HEAT AND MASS TRANSFER BY NATURAL CONVECTION

BAL M. MAHAJAN
Solar Equipment Group, National Bureau of Standards, Gaithersburg, MD 20899

Abstract—Experiments to measure the interzonal heat and mass transfer were carried out in two full size adjoining rooms under two different conditions. Before starting the tests, one of the rooms was heated to an average temperature of 32°C, while the other room was cooled to an average temperature of 19°C. To start the first type of tests, the auxiliary heating and cooling were turned off and the door blocking the opening opened. For the second test, auxiliary cooling was turned off, while the auxiliary heat was left on in the heated room. Visual observations of the flow phenomenon were made. Velocity and temperature profiles of the air-flow through the opening, and air temperatures in the test rooms were measured. The experimental mass and heat flow rates were computed from the velocity and temperature data and compared with the values predicted by the existing algorithms based on the application of the Bernoulli's equation. The agreement between the measured and predicted values is better for a value of discharge coefficient $C = 0.45$ than it is for $C = 0.611$ (the theoretical value of C for a sharp edged orifice quoted in the literature).

1. INTRODUCTION

Interzonal natural convection plays a major role in the distribution of heat in the passive solar buildings. The topic of interzonal heat and mass flow by natural convection via large openings has received considerable attention in the literature. Algorithms for estimating the interzonal mass and heat transfer have been developed[1–11]. However, data from controlled experiments in full size rooms and buildings needed to verify and improve these algorithms are very limited. Hence, experimental research to measure the interzonal mass and heat flow by natural convection via a doorway has been undertaken. The objectives of the initial study were to measure the velocity and temperature profiles of the air moving by natural convection through the doorway opening, to compute mass and heat transfer from the velocity data, and to compare the results with the values predicted by the simple existing algorithms.

The experiments were performed in the two adjoining rooms of the National Bureau of Standards' Passive Solar Test Facility under two different test conditions. This paper describes the experimental set-up, instrumentation, and measurement procedures used. The paper will present representative results and compare the measured data with values predicted by the algorithms.

2. THEORY

The simple development presented below follows the theory based on the application of the Bernoulli equation developed in [1–6]. Assuming that the flow is steady, and the zone-to-zone temperature difference, ΔT, is independent of the height above the floor, the magnitude u, of the local air velocity in the opening is given by:

$$u = C[2g(\Delta T/\bar{T})Y]^{0.5}, \tag{1}$$

where the quantity C is an aperture discharge coefficient, which accounts for the viscous losses at the area contraction. The theoretical value of C for a sharp edged orifice, such as a doorway, is equal to 0.611[1]. The discharge coefficient, however, varies with the boundary proportions and Reynold number for real flows. Furthermore, its value could be adjusted to account for other losses.

Equation (1) may be expressed in non-dimensional form as follows:

$$u/U_m = C[2Y/H]^{0.5}, \tag{2}$$

where

$$U_m = [gH\Delta T/\bar{T}]^{0.5}, \tag{3}$$

where U_m is the maximum possible velocity for an ideal flow for a given value of H, ΔT, and $\bar{T}$.

Considering the flow to be one-dimensional and perpendicular to the plane of the opening, the mass flow rate per unit door width, $\dot{m}$, may be given as follows:

$$\dot{m} = (C\bar{\rho}/3)\,[(gH^3\Delta T/\bar{T})]^{0.5}. \tag{4}$$

The value of $\bar{T}$ remains fairly close to 300°K, over the range of temperatures of interest for this study. Taking the value of $\bar{T}$ to be a constant and equal to 300°K, eqn (4) may be rewritten as:

$$\dot{m} = (C\bar{\rho}/3)\,[(gH^3/300)]^{0.5}\,(\Delta T)^{0.5}. \tag{5}$$

The associated rate of heat transfer per unit door width through the opening may be given by:

$$\dot{Q} = \dot{m}C_p\Delta T = (C\bar{\rho}C_p/3)\,[(gH^3/300)]^{0.5}\,(\Delta T)^{1.5}. \tag{6}$$

Equations (1)–(6) cannot be exact for real flow situations, because of the following effects. The flow of air in the opening is not one-dimensional, and the effects of viscosity may not be negligible. The ΔT in actual situations may not be independent of Y. Owing to the differences in the temperatures and densities of inflow and outflow air, the bulk velocity of inflow must be somewhat lower than that of the outflow in order to preserve the mass balance. Furthermore, the neutral plane, i.e., the plane of zero velocity, may not coincide with mid-height of the opening.

Some researchers have modified the simple algorithm to account for the temperature distribution in each zone and the shift of the natural plane[7, 8]. Some other theoretical developments model the inflow and outflow with different equations[9, 11]. However, in this paper we will compare the experimental data with the simple algorithm presented above.

3. EXPERIMENTAL SET-UP

The experiments were carried out at the NBS Passive Solar Test Facility. Figure 1 shows the floor plane of the test building. A complete description of the building is available in [12].

The rooms labeled cell #2 and cell #3 in the Fig. 1 building were used to perform the experiments. All direct solar radiation was blocked from entering the test cells, and the doorway opening connecting the two cells was fitted with a removable door. Each cell has a fan coil unit, as indicated in Fig. 1, for auxiliary heating and cooling. Four additional baseboard type electric heaters were also installed in cell #2; the location of these heaters is also indicated in Fig. 1. These heaters and the fan coil units were individually controlled by thermostats with a 0.5°C deadband.

Figure 2 is a schematic cross-section of the test rooms, showing dimensions of the doorway opening. Figure 2 also shows the location of the thermocouples installed to monitor the room air temperature in the test rooms. Four additional thermocouples were installed (Fig. 3) to monitor the air temperature at the top and bottom of the opening in each cell. Figure 3 shows a south elevation of the test area and the coordinates, and the schematic of the doorway opening is shown in Fig. 4. The air speed was measured with eight hot wire anemometers using temperature compensated hot wire probes. A specially designed rig permitted the placement of eight hot wire probes and eight thermocouples at any desired position in the opening.

The maximum overall uncertainty is estimated to be 0.5°C in the temperature measurement and 0.025 m/s in the air speed measurements.

3.1 *Test procedures*

Two types of tests were performed, for the first type of test, the position of the hot wire probes and the thermocouples placed in the opening were adjusted to the desired locations, and the doorway opening was blocked with a tight fitting removable door placed in cell #2. The heaters in cell #2 were turned on with thermostats set at 32°C, and the air conditioning thermostat in cell #3 was set at 19°C. The process of heating cell #2 and cooling cell #3 was continued for 6–10 hours.

About 10 minutes before the start of an experiment, heaters in cell #2 and air conditioning in cell #3 were turned off. The hotwire anemometers were turned on, and the door blocking the opening between the test rooms was removed to start the experiment. The experiment was continued for 5–7 hours. The same test procedures were followed for the second type of experiments; except that the baseboard heaters in cell #2 were left on, and these experiments were run for about 14–16 hour durations.

During both types of experiments, the sensors of the hot wire probes were so aligned as to measure the magnitude of the X-component of the air velocity. All of the sensors were scanned at two minute intervals. During some tests the temperature and velocity profiles of the air flowing through the

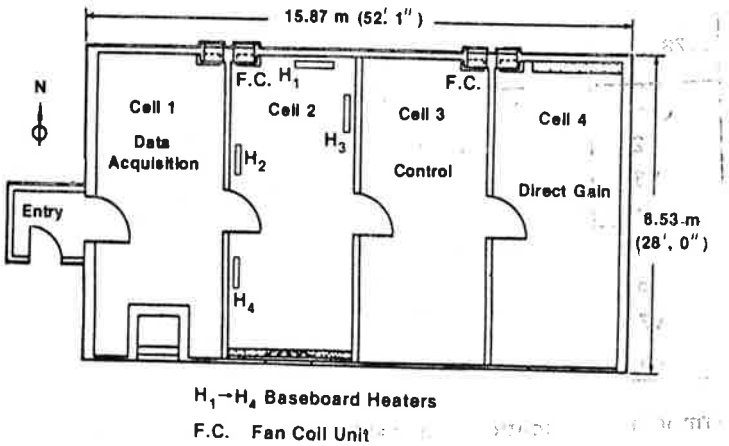

Fig. 1. Floor plan of the NBS passive solar test building.

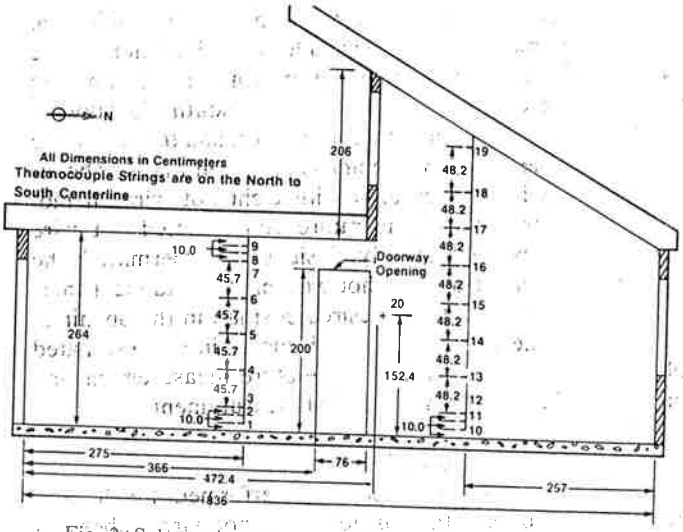

Fig. 2. Schematic east view of test cells showing location of air temperature sensors.

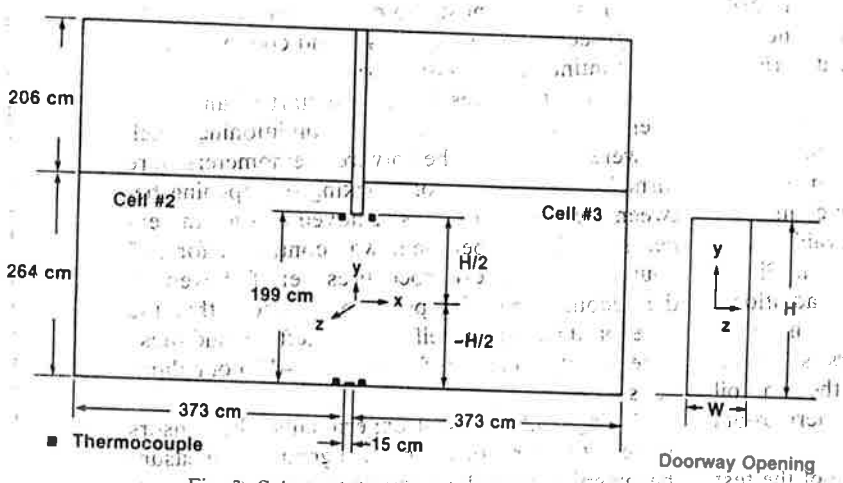

Fig. 3. Schematic south view of the test area.

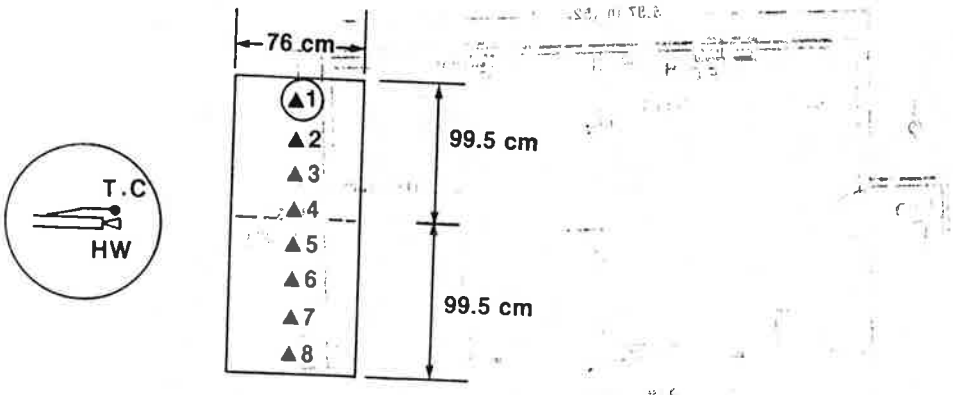

Fig. 4. Schematic of the doorway opening.

opening were monitored along the height of the opening, while during other tests these profiles were monitored along the width of the opening. During separate tests, visual observations of the flow phenomenon were made applying flow visualization techniques using smoke. Smoke was generated by several incense sticks placed at different locations in the opening and a video tape of the phenomenon for the first type of experiment was made.

4. TEST RESULTS AND DISCUSSION

4.1 *Visual observation*

The following observations were made during the flow visualization tests. The flow of air through the opening was three-dimensional with the X and Y velocity components appearing dominant. The flow was not symmetrical with respect to the openings mid-height, and the neutral plane (i.e., the plane of zero horizontal velocity) was shifted upwards. The air moving from the warmer to cooler room (outflow) via the upper portion of the opening had a significant upward velocity component, while the air moving from the cooler to the warmer room (inflow) had a downward velocity component. Using the hydraulic analogy, the outflow appeared as the up-side-down picture of water flow over a weir; while the inflow appeared as the flow under a sluice gate. The flow pattern observed here is different than those observed by Nansteel and Greif[4] because of the different geometry of the test set-up and test conditions.

Figure 5 is a photograph of a single frame of the flow visualization movie, it shows the streamlines of the outflow as seen from the cell #3 (the cool room). The streamlines visible in the figure were from incense sticks situated at a vertical distance of 0.9 ($H/2$), 0.6 ($H/2$) and 0.4 ($H/2$) from the mid-height of the opening.

4.2 *Air temperatures*

Typical air temperature data from different experiments are shown in Figs. 6–9. Figure 6 shows the temperature of outflow at various locations along the width of the opening for various elapsed times for the first type of test. These temperatures were measured at a vertical distance of $2Y/H = 0.93$ and at $X = 0$. These data indicate that the air temperature across the width of the opening is fairly uniform. The air temperature is decreasing with time since the air temperature in the warm room decays with time.

Figures 7 and 8 show the vertical profiles of air temperature in the two test rooms and in the doorway opening from the first type of test. These figures show the data for elapsed times of 10 minutes, and 5 hours, respectively. The data presented in Figs. 7 and 8 indicate that the room-to-room air temperature difference decreases with time as expected. The room-to-room temperature difference is fairly independent of the height above the floor.

Figure 9 shows the room-to-room temperature difference ($\Delta T = T_w - T_c$) for various elapsed times for four different tests; two of these tests are of the first type experiment, and the other two are of the second type of experiments. These data indicate that the value of ΔT drops rapidly during the first two hours and the rate of drop in the value of ΔT decreases with elapsed time, and ΔT becomes nearly constant after about 8 hours for the second type of test.

4.3 *Air velocities*

Typical data for the X-component of air velocity, u, from different experiments are shown in Figs.

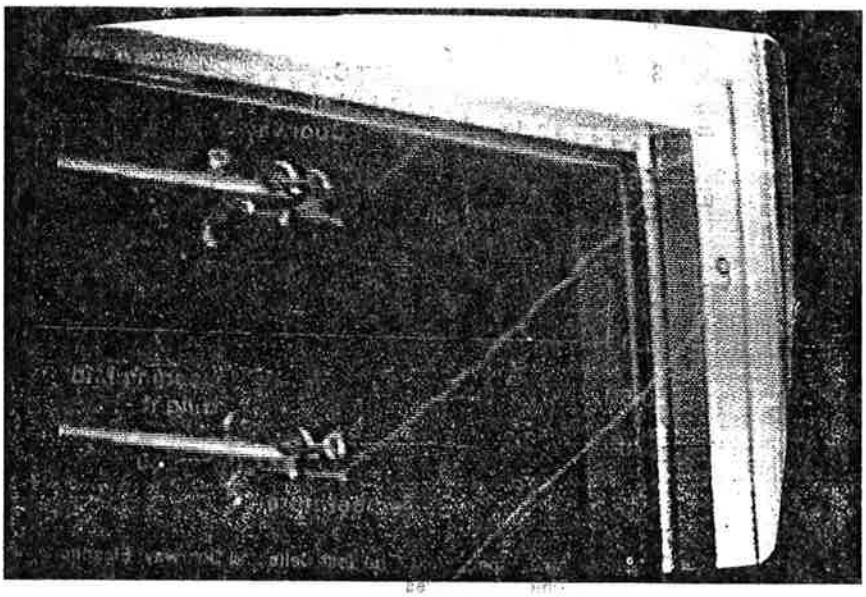

Fig. 5. A photograph showing streamlines of the outflow through the opening.

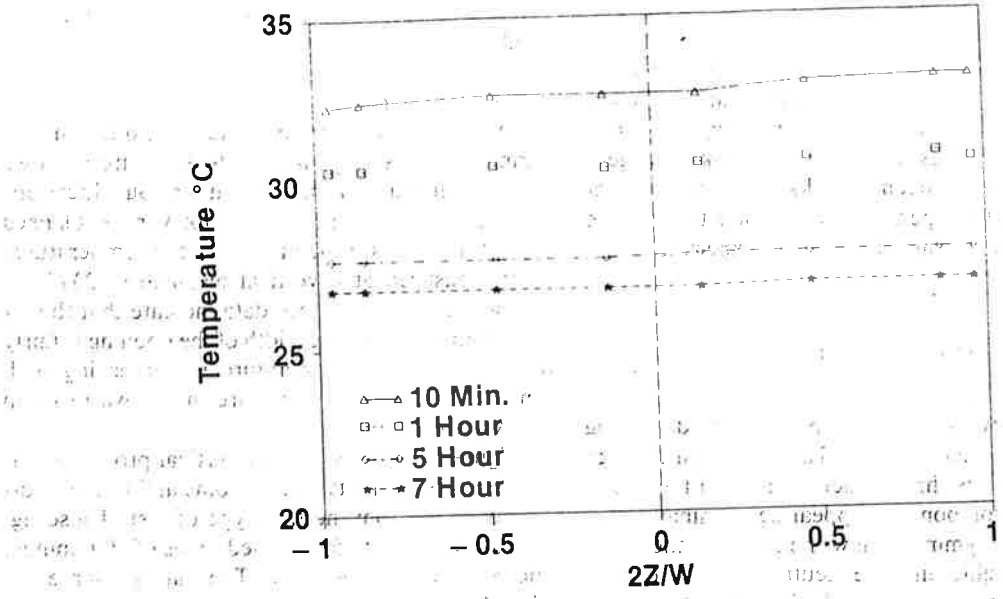

Fig. 6. Air temperature along the opening width at $x = 0$, $2y/H = 0.93$, for various elapsed times.

10–12. Figure 10 shows the magnitude of outflow velocity at various locations along the width of the opening for four elapsed times for the first type of test. These data indicate that the air velocity across the width of the opening was not as uniform as the temperatures. This non-uniformity of flow velocity across the width of the opening suggests the 3-dimensional nature of the flow and needs further investigation. The existing algorithms for estimating room-to-room mass and heat transfer do not account for this lateral variations of the flow velocity.

Figure 11 shows typical air velocity data at various distance along the height of the opening and at $X = 0$ and $Z = 0$, for various elapsed times. These data are reproduced in non-dimensional form in Fig. 12; for this purpose the measured value of local velocity was divided by the value of maximum ideal velocity computed by using the measured values of ΔT and $\bar{T}$. Equation (2) for $C = 0{,}61$ is also plotted on this figure for the purpose of comparison.

The data of Figures 11 and 12 indicate the following:

1. The velocity profile is not symmetrical with respect to the mid-height of the opening. For equal distances from the mid-height, the magnitude of the outflow velocity is larger than that of the inflow. This nonsymmetric velocity distribution is apparently due to the nonsymmetric boundary con-

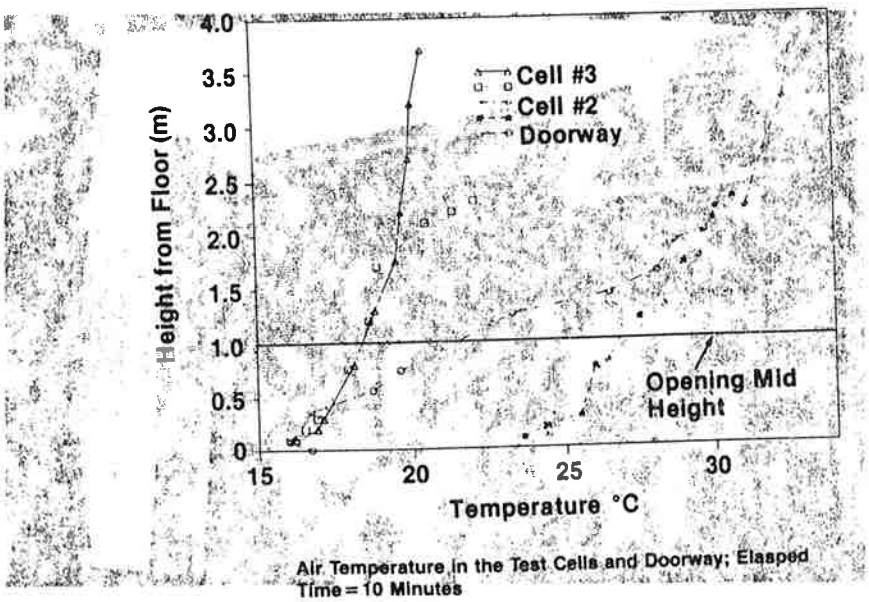

Fig. 7. Air temperature in the test cells and doorway; elapsed time = 10 minutes.

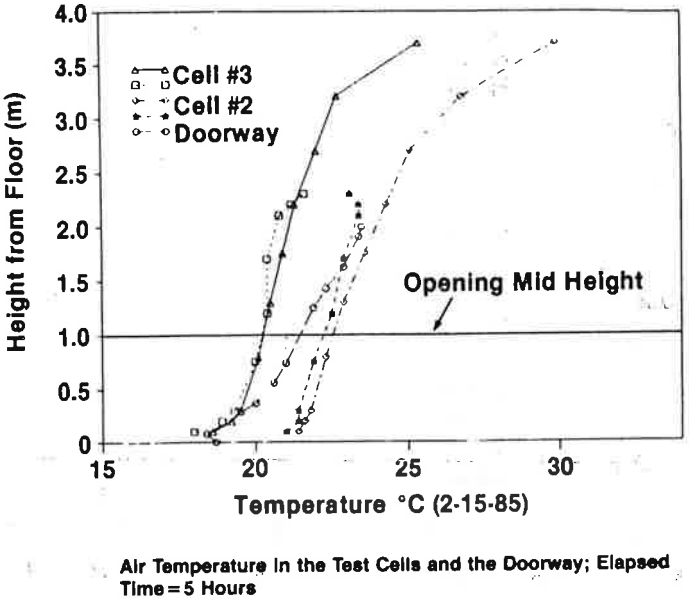

Fig. 8. Air temperature in the test cells and the doorway, elapsed time = 5 hours.

straints at the top and the bottom of the opening. The curving of the streamlines around the top edge of the opening probably results in higher velocities of the outflow than that predicted by eqn (1) or (2); while the presence of a floor (no slip constraint) modifies the inflow and the experimental velocities are lower than that predicted by the algorithm. The simple algorithm does not account for both of these constraints.

2. The zero velocity points (linearly interpolated) do not coincide with mid-height of the opening, suggesting that the plane of zero velocity (i.e., neutral plane) was not at the mid-height of the opening. Rather the neutral plane was generally above the mid-height. This upward shift of the neutral plane was also seen during flow visualization of the flow phenomenon.

4.4 *Mass and heat transfer rates*

The experimental mass inflow and outflow rates were computed from the velocity and temperature data taken at various distance along the height of the opening and at $X = Z = 0$. The local velocity was multiplied by local air density and the width of the opening to obtain the local mass flow rate. Integration of the local mass flow rate with respect to Y, from Y = neutral plane distance of $Y = H/2$, yielded the mass flow rate. This integration was

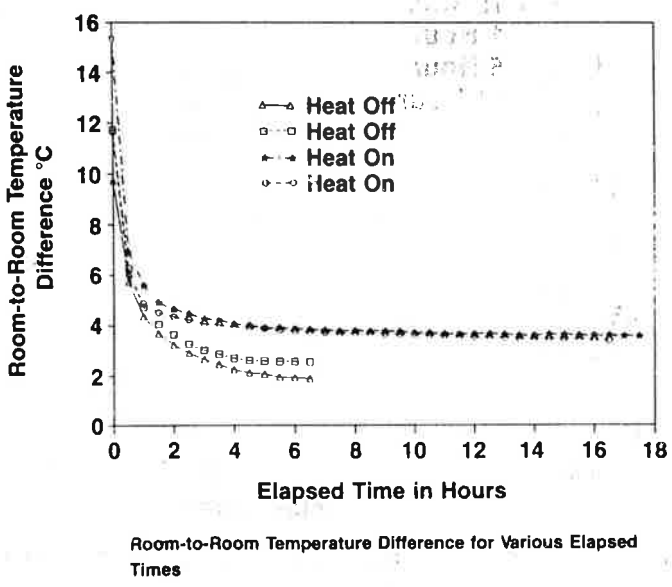

Fig. 9. Room-to-room temperature difference for various elapsed times.

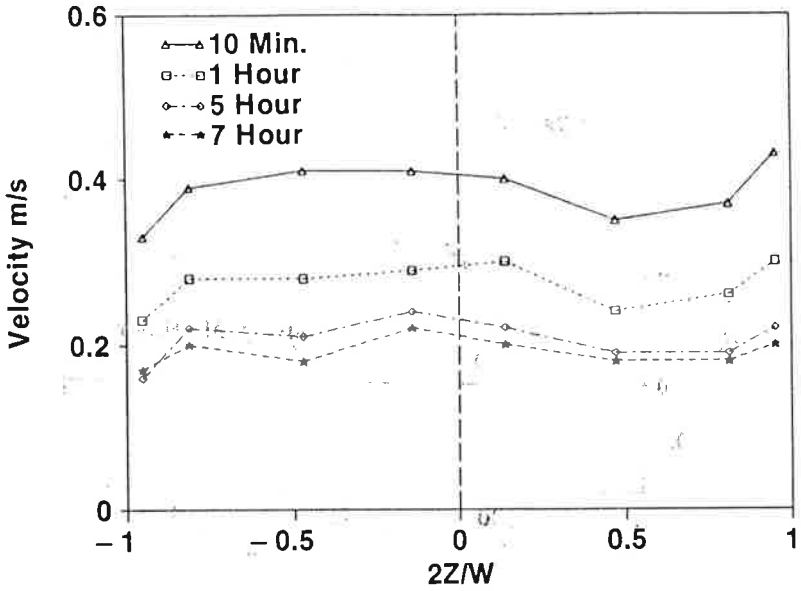

Fig. 10. Variation of velocity u, along the opening width at $x = 0$; $2y/H = 0.93$ for various elapsed times.

performed applying trapezoidal summation techniques. The neutral plane distance used for this purpose was obtained by linear interpolation of velocity data. The small difference (0–5%) in the values of inflow and outflow thus computed is attributable to unaccountable air infiltration elsewhere and non-uniformity of air speed across the width of the opening.

The rate of heat transfer through the door was obtained by multiplying the mass flow rate of the outflow with the specific heat of air, C_p, and measured value of ΔT. The rate of heat transfer through the common wall ($\dot{Q}_w$), depending on the value of ΔT, was about 10% or less when compared with the rate of heat transfer through the door ($\dot{Q}$). Using the value of unit thermal conductance of the common wall (0.29 W/(m^2 – °C) given in [12], the above mentioned ratio may be expressed as follows:

$$\dot{Q}_w/\dot{Q} \approx 0.045/C\sqrt{\Delta T} = 0.1/\sqrt{\Delta T} \qquad (7)$$

The experimental values of mass flow rate of the outflow as a function of square root of ΔT are shown in Fig. 13. The data presented are for two first type experiments and two second type experiments. Equation (5) for a value of $C = 0.61$ and C

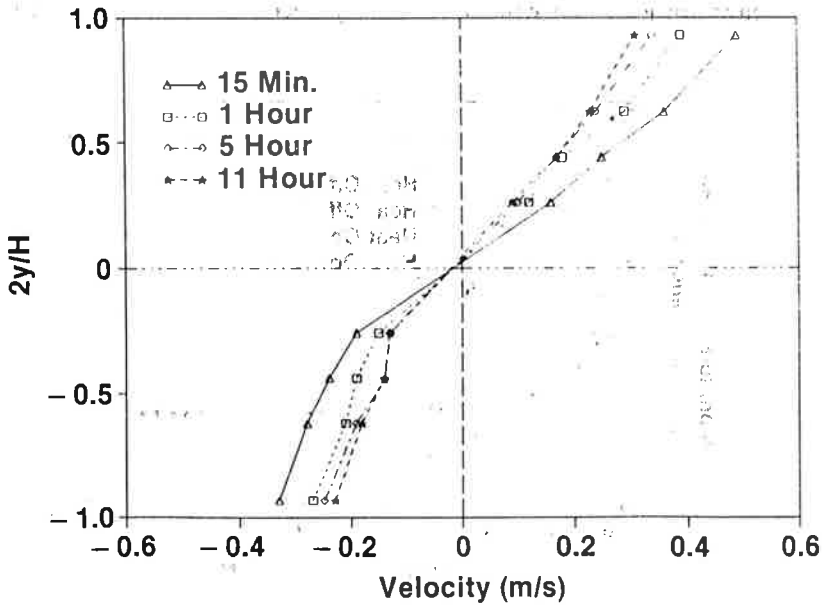

Fig. 11. Velocity u, along the opening height at $2 - z = 0$, for various elapsed times.

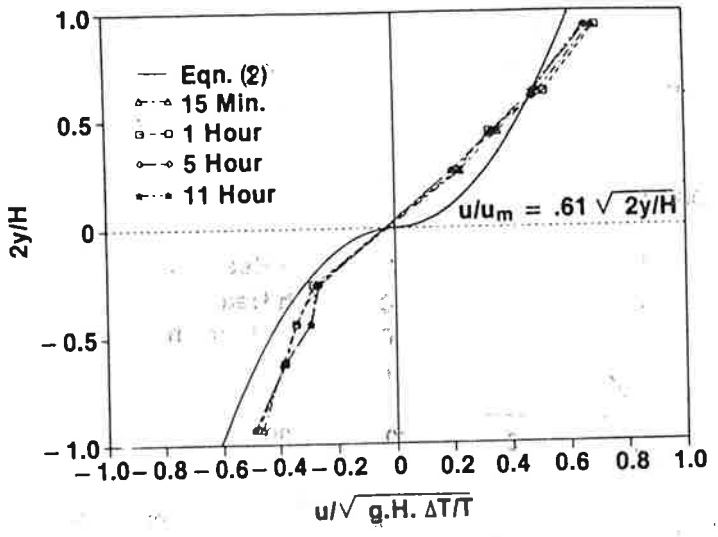

Fig. 12. Nondimensional velocity along the opening height at $x = z = 0$ for various elapsed times.

$= 0.45$ is also plotted on Fig. 13. The heat flow rate data for various values of ΔT, plotted as heat flow rate versus $\Delta T^{1.5}$, is shown in Fig. 14. Equation (6) for a value of $C = 0.61$, and $C = 0.45$ is also shown on this figure.

The data of Figs. 13 and 14 indicate that the mass and heat transfer rates follow the general trends depicted by eqn (5) and (6), respectively. However, the agreement between the measured and the predicted values is better for $C = 0.45$ than it is for $C = 0.61$. It appears that the value of discharge coefficient, $C = 0.611$, for a sharp edged orifice is not applicable to the present flow phenomena; this may be due to the particular geometric configuration of the present experimental set-up. The value of discharge coefficient ($C = 0.45$) is lower than the value of C indicated by other researchers. For example, Steckler *et al.*[10] obtained a value of $C = 0.68$, and Balcomb *et al.*[13, 5] indicated a value of $C = 0.611$ for volume or mass flow and $C = 0.9$ for heat flow. The difference in the values of C is apparently due to the differences in the experimental set-ups and test condition, and it requires further investigation.

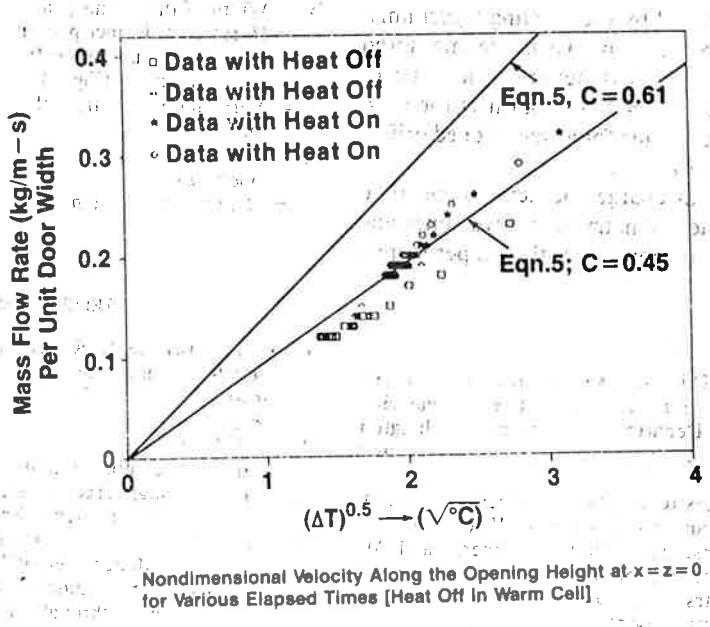

Fig. 13. Rate of mass transfer by natural convection across the doorway opening as a function of cell-to-cell temperature difference, ΔT.

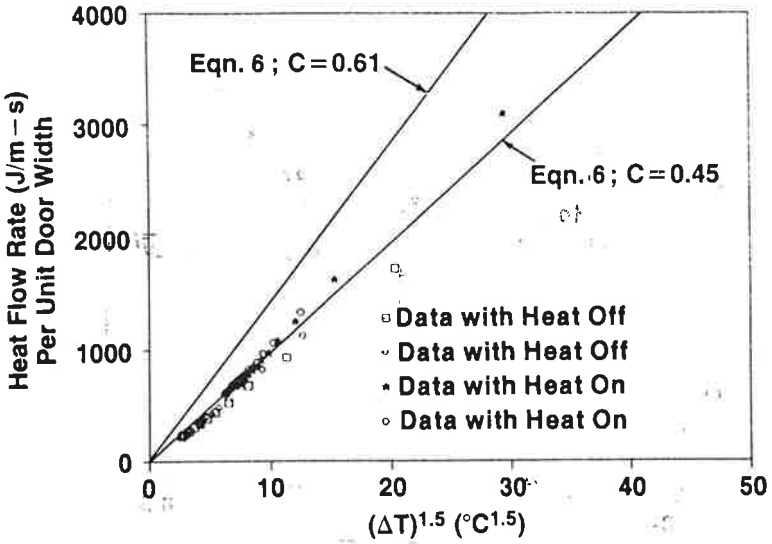

Fig. 14. Rate of heat transfer by natural convection across the doorway opening as a function of cell-to-cell temperature difference, ΔT.

5. CONCLUSIONS

Based on the data presented, the following conclusions may be drawn:

1. The room-to-room air flow by natural convection via a doorway opening is a three-dimensional flow phenomenon.
2. The velocity profile along the height of the opening is not symmetrical with respect to the mid-height of the opening.
3. The velocity of outflow is generally higher than that of the inflow, and the neutral plane does not coincide with mid-height of the opening. The velocity data do not agree with the values predicted by the existing algorithms.
4. The mass and heat transfer data follow the general trends depicted by the existing algorithms. However, the agreement between the measured and the predicted results is better for a value of discharge coefficient $C = 0.45$ than it is for $C = 0.611$ (the theoretical value for a sharp edged orifice suggested in the literature).
5. The value of discharge coefficient appears to be dependent on the geometry of the two zones and the apertures, and it requires further experimental investigation.

Acknowledgment—This work is sponsored by the Passive and Hybrid Solar Energy Division, Office of Solar Heat Technologies, U.S. Department of Energy, Washington, D.C. 20585, as part of the experimental systems research program.

The author wishes to express his sincere gratitude to Dr. Stanley T. Liu and Mr. George N. Walton for many valuable suggestions, Mr. Donn E. Ebberts and Mr. Thomas J. Bodine for valuable contributions in instrument installation, and Mrs. Flora J. Parsons for the timely preparation of the manuscript.

NOMENCLATURE

C = Discharge coefficient (non-dimensional)
C_p = Specific heat of air (W-s/kg-°C)
H = Height of the opening (m)
g = Acceleration due to gravity (m/s^2)
$\dot{m}$ = Mass transfer rate per unit door width (kg/m-s)
$\dot{Q}$ = Heat transfer rate per unit door width (W/m)
T_c = Average value of air temperature in the cool room (°C or °K)
T_w = Average value of air temperature in the warm room (°C or °K)
$\bar{T} = (T_c + T_w)/2$ (°K)
$\Delta T = (T_w - T_c)$, room-to-room temperature difference (°C or °K)
u = Magnitude of horizontal velocity (X-component) in the opening (m/s)
U_m = Magnitude of the maximum possible velocity for an ideal flow (m/s)
W = Width of the opening (m)
X = Horizontal distance perpendicular to the plan of the opening and measured from the mid-thickness of the opening (m) (Fig. 4)
Y = Vertical distance from the mid-height of the opening (m)
Z = Horizontal distance from the mid-width of the opening (m)
ρ = Density of air (kg/m^3)

REFERENCES

1. W. G. Brown and K. R. Solvason, Natural convection through rectangular openings in partitions—1 vertical partitions. *Int. J. Heat and Mass Transfer* **5**, 859 (1962).
2. B. H. Shaw, Heat and mass transfer by natural convection and combined natural convection and forced air flow through large rectangular openings in a vertical partition. Int. Mech. Eng. Conference on Heat and Mass Transfer by Combined Forced and Natural Convection. Manchester (1971).
3. D. D. Weber, Similitude modeling of natural convection heat transfer through an aperture in passive solar

heated building. LASL Report LA-8385-T. Los Alamos National Laboratory, Los Alamos, New Mexico (1980).
4. M. W. Nansteel and R. Greif, Natural convection in undivided and partially divided rectangular enclosures. *T. of Heat Transfer* **103** (1981).
5. J. D. Balcomb and K. Yamaguchi, Heat distribution by natural convection. *Proc. Eighth National Passive Solar Conference*, Santa Fe, New Mexico, Sept. 5–10 (1983).
6. G. N. Walton, A Computer algorithm for estimating infiltration and inter-room air flow. NBSIR 83-2635 National Bureau of Standards, Gaithersburg, Maryland (1982).
7. D. Hill, A. Kirkpatrick and P. Burns, Interzonal natural convection heat transfer in a passive solar building. ASME/AICHE National Heat Transfer Conference, Denver, CO (1985).
8. G. F. Jones, J. D. Balcomb and D. R. Otis, A model for thermally driven heat and air transport in passive solar buildings. ASME Winter Annual Meeting, Miami Beach, Florida (1985).
9. J. A. Quintiere and K. DenBraven, Some theoretical aspects of fire induced flows through doorways in a room-corridor scale model. NBS Report NBSIR 78-1512 (1978).
10. K. D. Steckler, J. A. Quintiere and W. J. Rimkinsen, Flow induced by fire in a compartment. Nineteenth Symposium International on Combustion/The Combustion Institute, Haifa, Israel (1982).
11. J. Prahl and H. W. Emmons, Fire Induced Flow Through an Opening. *Combustion and Flame* **25**, 369–385 (1975).
12. B. M. Mahajan, National bureau of standards passive solar test facility-instrumentation and site handbook. NBS Report NBSIR 84-2911 (1984).
13. J. D. Balcomb, G. F. Jones and K. Yamaguchi, Natural air motion and stratification in passive buildings. *Proceedings of the Passive and Hybrid Solar Energy Update*, Washington, D.C., Sept. 5–7 (1984).